

RESEARCH

Open Access



Dietary selection of distinct gastrointestinal microorganisms drives fiber utilization dynamics in goats

Xiaoli Zhang^{1,2}, Rongzhen Zhong³, Jian Wu¹, Zhiliang Tan^{1,4} and Jinzhen Jiao^{1,4*}

Abstract

Background Dietary fiber is crucial to animal productivity and health, and its dynamic utilization process is shaped by the gastrointestinal microorganisms in ruminants. However, we lack a holistic understanding of the metabolic interactions and mediators of intestinal microbes under different fiber component interventions compared with that of their rumen counterparts. Here, we applied nutritional, amplicon, metagenomic, and metabolomic approaches to compare characteristic microbiome and metabolic strategies using goat models with fast-fermentation fiber (FF) and slow-fermentation fiber (SF) dietary interventions from a whole gastrointestinal perspective.

Results The SF diet selected fibrolytic bacteria *Fibrobacter* and *Ruminococcus* spp. and enriched for genes encoding for xylosidase, endoglucanase, and galactosidase in the rumen and cecum to enhance cellulose and hemicellulose utilization, which might be mediated by the enhanced microbial ATP production and cobalamin biosynthesis potentials in the rumen. The FF diet favors pectin-degrading bacteria *Prevotella* spp. and enriched for genes encoding for pectases (PL1, GH28, and CE8) to improve animal growth. Subsequent SCFA patterns and metabolic pathways unveiled the favor of acetate production in the rumen and butyrate production in the cecum for SF goats. Metagenomic binning verified this distinct selection of gastrointestinal microorganisms and metabolic pathways of different fiber types (fiber content and polysaccharide chemistry).

Conclusions These findings provide novel insights into the key metabolic pathways and distinctive mechanisms through which dietary fiber types benefit the host animals from the whole gastrointestinal perspective.

Keywords Gastrointestinal microorganisms, Fiber utilization process, Short-chain fatty acids, Cobalamin biosynthesis, Fiber types

Background

According to the Food and Agriculture Organization of the United Nations, the areas of meadows and pastures were reduced by 209 million ha, and the cropland area per capita was decreased by 17% from 2002 to 2022 [1]. Simultaneously, 152 million more people faced hunger in 2023 when compared to 2019, and the projections show 582 million people will suffer from chronic undernourishment in 2030 [2]. Hence, in a world of finite biological resources, urgent coordinated actions are imperative to transform agri-food systems that would enable producing food with human-unavailable biomass such as plant

*Correspondence:

Jinzhen Jiao

jjz@isa.ac.cn

¹ State Key Laboratory of Forage Breeding-By-Design and Utilization, Institute of Subtropical Agriculture, Chinese Academy of Sciences, Changsha, Hunan 410125, China

² College of Animal Science and Technology, Southwest University, Chongqing 400715, China

³ Jilin Province Feed Processing and Ruminant Precision Breeding Cross Regional Cooperation Technology Innovation Center, Northeast Institute of Geography and Agroecology, Chinese Academy of Sciences, Changchun 130102, China

⁴ Yuelushan Laboratory, Changsha, Hunan 410128, China



© The Author(s) 2025. **Open Access** This article is licensed under a Creative Commons Attribution-NonCommercial-NoDerivatives 4.0 International License, which permits any non-commercial use, sharing, distribution and reproduction in any medium or format, as long as you give appropriate credit to the original author(s) and the source, provide a link to the Creative Commons licence, and indicate if you modified the licensed material. You do not have permission under this licence to share adapted material derived from this article or parts of it. The images or other third party material in this article are included in the article's Creative Commons licence, unless indicated otherwise in a credit line to the material. If material is not included in the article's Creative Commons licence and your intended use is not permitted by statutory regulation or exceeds the permitted use, you will need to obtain permission directly from the copyright holder. To view a copy of this licence, visit <http://creativecommons.org/licenses/by-nc-nd/4.0/>.

cell wall carbohydrates [3]. Ruminants, such as goats, cattle, and sheep, are distinguishable from monogastric animals due to their capacity to convert plant cell wall fibers into high-quality animal products such as milk and meat [4], as a consequence, producing the ruminant products consumes fewer grain resources [5]. Of particular interest, in addition to the significance of providing beneficial nutrients such as healthy unsaturated fatty acids and bioactive phospholipids [6, 7], caprine agriculture is particularly well-suited for small-scale agricultural operations and has better tolerance to poor environmental conditions [8].

The complex rumen microbial ecosystem, including bacteria, archaea, protozoa, and fungi [9], has been an immense source of diverse enzymes for plant polysaccharide depolymerization [10]. Generally, the abundant and recalcitrant sugar polymers of plant cell walls are primarily depolymerized into small oligosaccharides, with the aid of various and synergistic enzymes possessed in specialist cellulolytic and hemicellulolytic rumen microorganisms, including endoglucanase, cellobiohydrolase, α -glucosidase, and β -xylosidase [11]. Secondly, the soluble oligosaccharides are imported into microbial cells and metabolized through Embden–Meyerhoff–Parnas pathway and pentose phosphate pathway for utilization of hexoses and pentoses. Finally, these sugars are fermented into short-chain fatty acids (SCFAs), CO_2 , and H_2 by most members of the rumen microbiome [4]. In addition, recent studies emphasize the importance of hydrogen as a key molecule in the rumen ecosystem with regard to methane production and community dynamics [12], and dietary selection of metabolically distinct microorganisms drives hydrogen metabolism and energy harvesting strategy in ruminants [13]. Despite this progress, the mechanism underlying the cross-feeding and metabolic interactions among different rumen microorganisms is still an unsolved mystery. Furthermore, microbial processes responsible for degradation of plant polysaccharides have been less explored in the intestine [14], where fiber digestion could be compensated by increased microbial fermentation in the hindgut in response to fiber-rich diets [15]. Therefore, it is in urgent need to decipher the dynamic enzymatic hydrolysis of plant polysaccharides from a whole gastrointestinal perspective.

Cobalamin, also known as vitamin B_{12} , represents an indispensable microelement in living organism for its role as a cofactor in various of physiological processes [16], especially in carbon processing and energy metabolism [17]. Since its de novo biosynthesis is an energetically expensive process involving over thirty enzymatic steps, cobalamin can only be synthesized by a small subset of prokaryotic organisms [18]. In light of large-scale metagenomic analyses, 675 genomes related to

cobalamin biosynthesis were recovered from the gastrointestinal microbes of ruminants, with 53 genomes contain complete cobalamin de novo biosynthesis genes [19]. Jiang et al. [19] pointed out the decreased abundance of *Fibrobacter* spp., a major agent of cobalamin biosynthesis, might contribute to the reduction of cobalamin biosynthesis potential after feeding high-grain diet, indicating that dietary fiber is vital for cobalamin biosynthesis. These arise to systematic research into microbial responses of cobalamin biosynthesis to dietary fiber components as well as its impact on the degradation of plant polysaccharides in the gastrointestinal tracts of ruminants.

To address the knowledge gap, we developed a gastrointestinal model of fast-fermentation fiber (FF) and slow-fermentation fiber (SF) selected microbiome. It is hypothesized that different dietary fiber types (fiber content and polysaccharide chemistry) could select distinct fiber degradation processes in the GIT microbiome, which might be modulated by microbial cobalamin biosynthesis. The microbial compositions and functional potentials were depicted using amplicon sequencing and metagenomic profiling, with emphasis on carbohydrate metabolism and cobalamin biosynthesis pathways. Their metabolic links were further deciphered and verified with differential assembled bins. This study emphasizes that dietary interventions modulate GIT microbial composition and in turn fiber degradation, which are closely linked to energy and cobalamin metabolism.

Methods

Animals and experimental design

All the procedures of this study were carried out following the guidelines approved by Animal Care and Use Committee of the Institute of Subtropical Agriculture, Chinese Academy of Sciences (approval No. ISA-R-2020-16). A total of 24 healthy native Xiangdong black goats (4.5 ± 0.4 month of age; 11.8 ± 0.6 kg) were used in present study and raised in individual pens in a well-ventilated room. Goats were randomly allocated to one of two dietary treatments, being a fast-fermentation fiber (FF) and a slow-fermentation fiber (SF), with 12 goats per treatment (Fig. 1A). The FF diet was formulated with 60% of peanut vine (in vitro rumen digestibility of 76% after 72 h incubation) as the forage, while the SF diet included 60% of sorghum straw (in vitro rumen digestibility of 54% after 72 h incubation) as the forage. Because these two diets exhibited remarkable variations in the apparent fiber digestion rate, hence referred as FF and SF diets. It is worth noting that the FF and SF diets differed substantially in fiber content (neutral detergent fiber, NDF, 33.0% vs. 45.6%) and polysaccharide chemistry (the amounts of cellulose, hemicellulose, and pectin; 16.6%, 10.1%, 3.4%

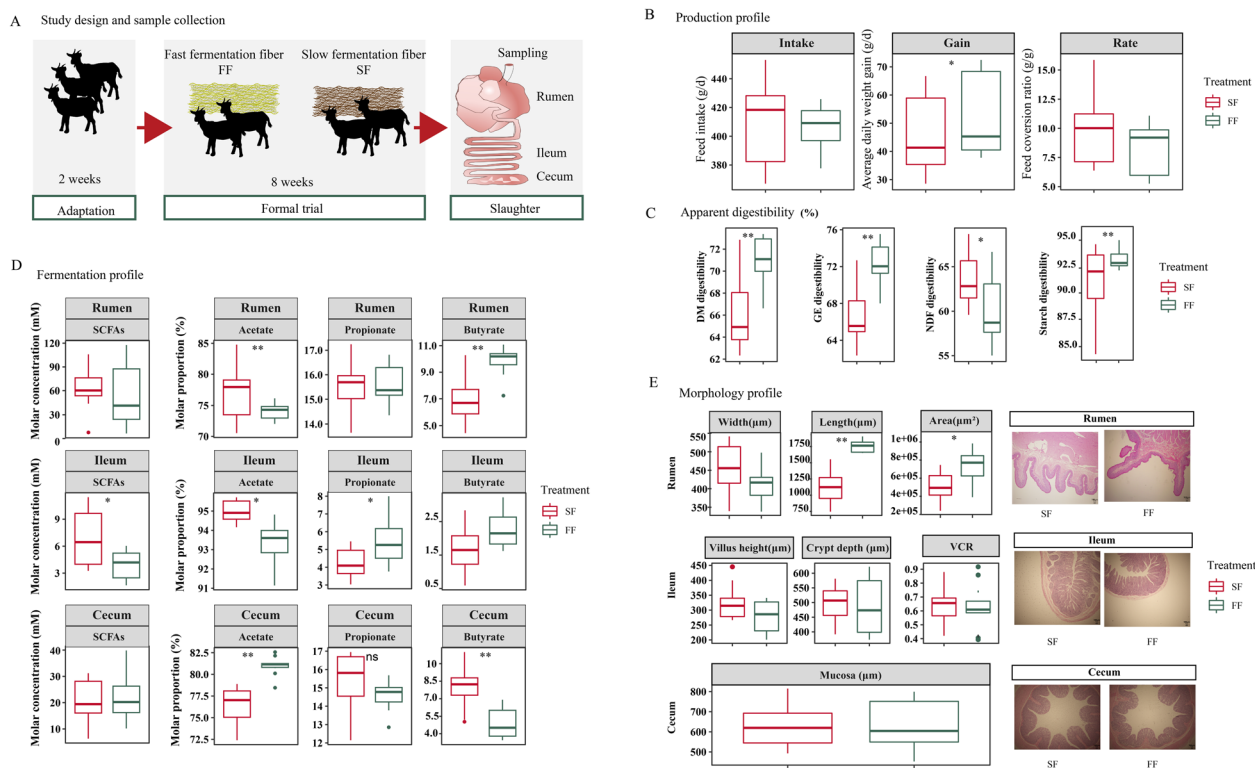


Fig. 1 Fast- and slow-fermentation fiber diets exhibit distinct growth performance, nutrient digestibility, GIT fermentation and morphology in goats. **A** Overview of design and sample collection. **B** Daily intake and weight gain. **C** Nutrient digestibility. **D** SCFA profiles in the rumen, ileum, and cecum. **E** Inspection of morphology changes in the rumen, ileum, and cecum. FF, fast-fermentation fiber; SF, slow-fermentation fiber. Asterisks denote significant *P* values, **P* < 0.05; ***P* < 0.01

vs. 22.8%, 13.7%, 1.3%, respectively, Table S1). Diets were offered ad libitum during the first 2 weeks for acclimation. During the formal experiment of 8 weeks, goats were fed twice daily (8:30 am and 6:00 pm) with 95% of the ad libitum dry matter (DM) intake to minimize diet selection. Feed refusals, if present, were collected and measured. All animals had free access to clean water during whole period. Two goats were eliminated from FF treatment due to illness (caught a cold and loss of appetite) and not included in the sampling process.

Sample collection

Total feces from each goat were gathered at 08:00 AM each day during last week of the experiment, with an adjustable stainless-steel screen positioned beneath each pen to facilitate complete fecal collection. At 08:00 AM each day, total feces per goat were weighed, mixed in a commercial concrete mixer, and 20% of the individual total daily feces were sampled using the coning and quartering method [20]. The representative fecal samples per goat were stored at -20°C for nutrient digestibility analysis.

Goats were humanely slaughtered after fasting for 12 h at the end of experimental period, and the gastrointestinal samples were collected within 15 min following slaughter. Ruminal content samples were collected from five locations in the rumen (the anterior dorsal, anterior ventral, medium ventral, posterior dorsal, and posterior ventral locations) and combined to represent a homogeneous sample [21]. The ileal and cecal content samples were collected from middle region of the respective intestine. A subsample (approximately 2 g) of content was placed in a 2-ml sterilized centrifuge tube, frozen in liquid nitrogen immediately, and then stored at -80°C for microbial analysis. Another subsample was acidified with 25% (w/v) metaphosphoric acids, the stored at -20°C for SCFA analysis [22]. Similarly, three pieces of full-thickness tissue samples excised from the ventral sac of the rumen, middle of the ileum and cecum, respectively. Each of samples were cut into 2 cm \times 2 cm pieces and fixed in 4% formaldehyde for 24 h followed by embedding in paraffin wax as described previously [23]. Afterwards, the sample-embedded wax was sliced into 4–5 μm thick sections followed by mounting onto poly-l-lysine-coated

glass slide, and then stored at 4 °C until further morphological analysis.

Sample analysis

The digestibility of DM, NDF, starch, and gross energy (GE) was determined as described as detailed previously [24], with acid-insoluble ash as an internal marker. The concentration of SCFAs (acetate, propionate and butyrate) in the content of rumen, ileum and cecum were determined by a gas chromatograph (Agilent 7890 A, Agilent Inc., Palo Alto, CA) according to the method described by Zhang et al. [22]. The morphological profile of gastrointestinal tracts was measured according to the procedures established by Tian et al. [23], with a minimum of 20 intact papillae or villi for each sample.

Microbial DNA and RNA extraction

Microbial DNA from ruminal, ileal and cecal content samples was extracted using the repeated bead beating method followed by extraction with the QIAamp Fast DNA Stool Mini Kit (Qiagen GmbH, Germany) as described in Zhang et al. [22]. The RNA was isolated using the RNeasy Mini Kit (QIAGEN) with the DNase I optional step according to the manufacturer's protocol [25]. The quantity of resultant DNA and RNA were measured on the Qubit fluorometer using the Qubit™ dsDNA BR assay/RNA HS assay (Thermo Fisher Scientific, Waltham, USA). The RNA quality was measured using an Agilent 2200 TapeStation (Agilent Technologies, Santa Clara, USA), and only samples with RNA integrity number ≥ 7.0 were used for generating amplicon libraries.

Amplicon analysis

The RNA was reverse transcribed to cDNA using the Prime-Script 1st Strand cDNA Synthesis Kit (Takara, Japan) [22]. For each DNA and cDNA sample, the full-length 16S rRNA gene was amplified using the universal primers F27 (5'-AGAGTTTGATCMTGGCTCAG- 3') and 1492R (5'-ACCTTGTTACGACTT- 3') [26]. The amplicon products were purified using QIAquick Gel extraction Kit (Qiagen, Hilden, Germany). The amplicon library was constructed using the SMRT Bell™ template prep kit 3.0 (Pacific Biosciences, USA) following the manufacturer's guidelines. Sequencing was performed according to JGI's standard procedures using the PacBio sequel II platform [27].

The DNA- and RNA-based amplicon sequences for bacterial diversity were analyzed according to the protocol previously described by Wu et al. [24]. Briefly, singletons were removed, and the amplicon sequence variants (ASVs) was clustered by USEARCH (v.11.0.667) with the method of unoise3 based on the reference database of SILVA (v.132) [28]. The taxonomy was obtained using the

RDP classifier (v.16) assignment with a 0.80 confidence threshold. Alpha and beta diversities were carried out on R (v.4.1.3) using package vegan (v.2.6–2).

Metagenomic analysis

Microbial genomic DNA (1.0 µg) was used to construct pair-ended metagenomic libraries using the TriSeq DNA PCR-Free Library Preparation Kit (Illumina, CA, USA). The library was sequenced on an MGISEQ- 2000 at the BGI Genomics Co., Ltd (Shenzhen, China). Approximately 28.8 GB of raw sequencing data were generated for each sample (Tables S2 and S3). Metagenomic sequencing reads were filtered to remove adapter and low-quality reads by Trimmomatic [29]. Reads that matched the host genome (*Capra hircus* ARS1) with BWA-MEM algorithm were removed and clean reads were obtained. Afterward, the clean reads from each sample were de novo assembled using MEGAHIT with “-min-contig-len 500” parameters [30]. The open reading frames of assembled contigs were predicted using Prodigal software (v2.6.3). Predicted gene catalogue was functionally annotated against the Kyoto Encyclopedia Genes and Genomes (KEGG) pathways using BLASTX, and screened for candidate CAZymes profiles using DIAMOND [31]. The abundances of KEGG Orthologies (KOs) and CAZymes were normalized into transcripts per million reads (TPM) prior to downstream analysis.

Metagenomic binning

MaxBin (v.2.2.4) [32], MetaBAT2 (v.2.11.1) [33], and CONCOCT (v.0.4.0) [34] were used for metagenomic binning based on assembled contigs with default parameters [35]. The bins generated from three approaches were integrated using the DAS tool (v.1.1.1) [36]. After filtering with completeness $\geq 90\%$ and contamination $\leq 5\%$, dereplicating at an average nucleotide identity (ANI) by dRep (v.2.5.4), 1030 MAGs was retained. These MAGs were predicted using the METAProdigal [37] and taxonomically annotated using GTDB-Tk (v.0.1.6) based on the Genome Taxonomy Database [38]. The abundance of MAGs in each sample was estimated using metaWRAP (v.1.3) with a “quant_bins” module [39]. A phylogenetic tree of the specific MAGs was built with PhyloPhlAn (v.1.0) [40] and visually inspected using iTol (v.4.3.1) [41].

Statistical analysis

All statistical analysis and image visualization were carried out in R software (version 4.1.3). The data of phenotype traits including growth performance, digestibility, GIT morphology, and SCEFA profiles between two dietary treatments were normally distributed and of equal variance and thereafter analyzed using one-way ANOVA.

Alpha diversities including Shannon and Chao1 indexes which did not conform to the normal distribution were analyzed using the Wilcoxon test. Ordination analysis of Bray–Curtis distance between two treatments from amplicon and metagenomic data were visualized using principal coordinate analysis and assessed using the PERMANOVA with 999 permutations. The taxonomic and functional profiles of GIT microbiome were compared between two treatments using the Wilcoxon rank-sum test. The P values were adjusted using the false discovery rate (fdr) correction, and a P -value < 0.05 was regarded as statistically significant.

Results

Gastrointestinal fermentation pattern was modulated by fiber types in a region dependent manner

In terms of animal performance, the average daily weight gain was greater (56.7 g/d vs. 42.1 g/d) in the FF treatment than that of SF treatment ($P < 0.05$, Fig. 1B). Goats in FF treatment exhibited greater DM, GE, and starch digestibility ($P < 0.05$), while goats adapted to the SF diet had greater NDF digestibility ($P < 0.05$, Fig. 1C). Insights from SCFA profiles indicated that as contrasted to the SF treatment, acetate molar proportion was reduced, while butyrate molar proportion was elevated in the rumen of FF goats ($P < 0.05$, Fig. 1D). In the ileum, SCFA concentration and acetate molar proportion were lower, while propionate molar proportion was greater in the FF goats ($P < 0.05$). Intriguingly, acetate molar proportion was greater, while butyrate molar proportion was lower in the cecum of goats adapted to FF diet. Furthermore, the absorption capacity of rumen epithelium was enhanced by FF treatment, as indicated by greater length and cross-section of ruminal papillae (Fig. 1E, $P < 0.05$). In summary, dietary fiber types differentially shifted GIT fermentation pattern in a region dependent manner.

Different bacterial taxa were enriched by dietary fiber types in the GIT

Sixty-six content samples covering rumen, ileum, and cecum from 22 goats fed FF or SF diet were analyzed for total (DNA-level) and metabolically active (RNA-level) microorganisms using full-length amplicon analysis. Only the alpha diversity of active bacterial community in the cecum was affected by dietary fiber types, as reflected by decreased Chao1 and Shannon indexes in the FF diet in comparison to SF diet ($P < 0.05$, Fig. 2A). At both DNA- and RNA-levels, samples were partitioned into three distinct clusters according to beta diversity analysis, corresponding to different physiological GIT regions, which was constrained by fiber types ($P_{GIT} < 0.001$, $P_{treatment} = 0.149$, $P_{GIT*treatment} = 0.079$ at DNA-level; $P_{GIT} < 0.001$, $P_{treatment} = 0.005$, $P_{GIT*treatment} = 0.015$ at

RNA-level, Fig. 2B). Concretely, bacterial diversity was distinguished by dietary fiber types in almost all GIT regions at both DNA- and RNA-levels ($P < 0.05$, Fig. 2C), except for total bacteria in the rumen ($P = 0.427$).

The compositions of dominant bacterial taxa were modified by dietary fiber types in a region dependent manner ($P < 0.05$, Fig. 2D). Specifically, in the rumen, when contrasted to FF treatment, SF treatment increased the abundances of *Saccharofermentans* and *Ruminococcus* at the DNA-level, and *Saccharofermentans*, *Pseudobutyrvibrio*, and *Fibrobacter* at the RNA-level ($P < 0.05$) while decreased the abundances of *Succiniclaticum* and *Mogibacterium* at the RNA-level ($P < 0.05$). In the ileum, abundances of *Clostridium_sensu_stricto* and *Clostridium_XI* were greater in the SF treatment at the DNA-level, but abundances of *Mogibacterium*, *Bifidobacterium*, and *Subdivision5_genera_incertae_sedis* were greater in FF treatment at the RNA-level ($P < 0.05$). In the cecum, SF treatment increased *Bacteroides* abundance while decreased *Akkermansia* abundance at both DNA- and RNA-levels ($P < 0.05$). These differential bacterial taxa were verified at species level based on the metagenomic data using kraken2, including *Ruminococcus* spp., *Butyrvibrio* spp., and *Bacteroides* spp. (Fig. S1). Furthermore, these taxa were significantly correlated with digestibility and fermentation parameters in the corresponding GITs; for example, ruminal *Ruminococcus* was positively correlated with acetate molar proportion and NDF digestibility, and cecal *Bacteroides* was positively correlated with NDF digestibility ($P < 0.05$, Fig. S2). Collectively, region-specific selections of microbial taxa were enriched by different dietary fiber types (fiber content and polysaccharide chemistry) and thus associated with distinct substrate preferences and degradation abilities.

Distinct pathways of fiber depolymerization were selected by two diets

Metagenomic analysis revealed that the richness index based on the non-redundant microbial gene catalogue was increased in the rumen and cecum in the FF treatment when compared to the SF treatment ($P < 0.05$, Fig. 3A). Principal coordinate analysis (PCoA) based on Bray–Curtis distance showed dietary fiber types selected distinct metabolic functions in each GIT region ($P < 0.05$, Fig. 3B). Intriguingly, “metabolism pathway” was the most abundant category affected by dietary fiber types, in particular “carbohydrate metabolism,” “xenobiotics biodegradation and metabolism,” “glycan biosynthesis and metabolism,” and “cofactors and vitamins” in the rumen ($P < 0.05$, Fig. S3). Meanwhile, “global and overview maps” and “xenobiotics biodegradation and metabolism” pathways were affected by dietary fiber types in the cecum ($P < 0.05$, Fig. S3).

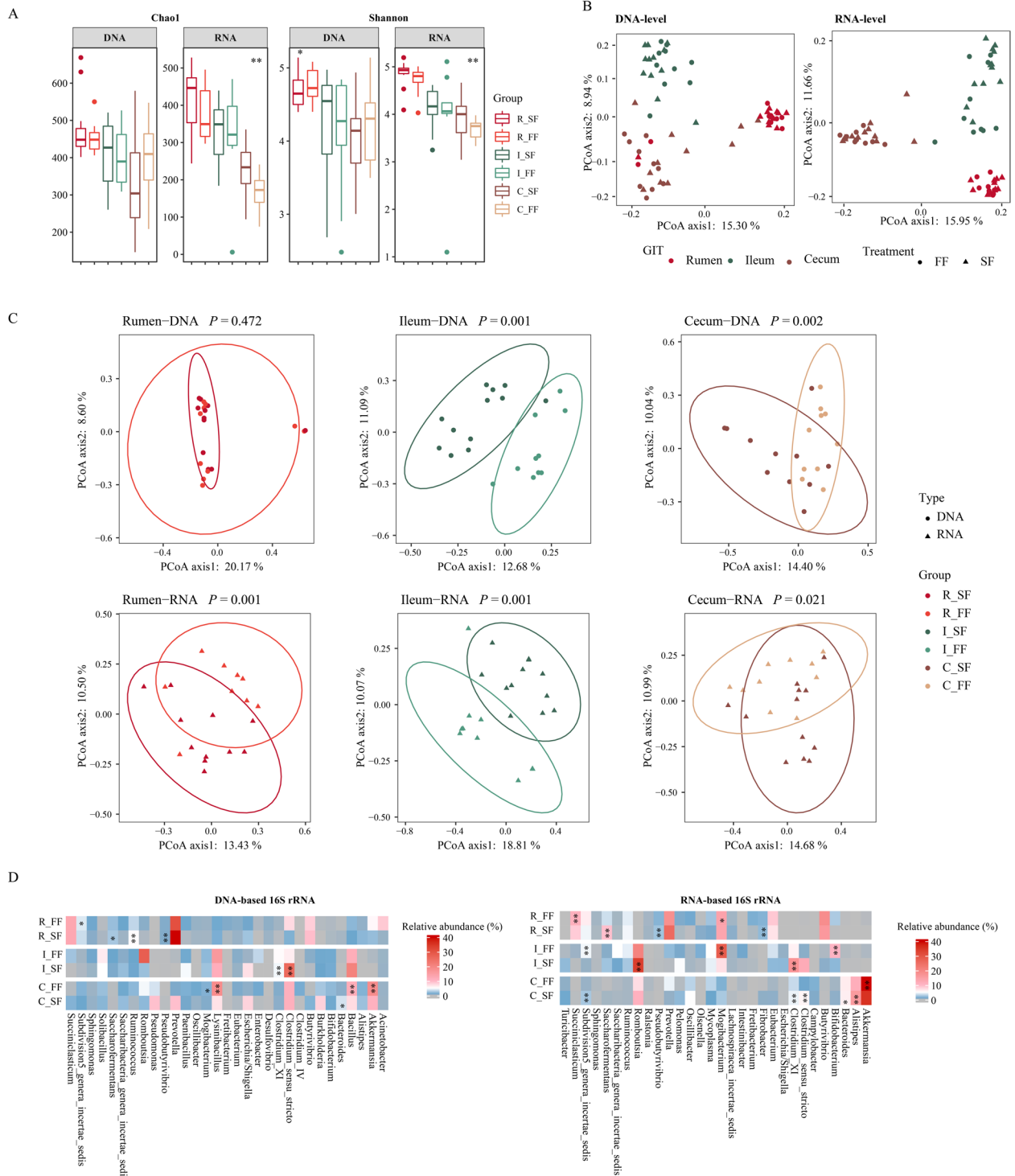


Fig. 2 Fast- and slow-fermentation fiber diets select distinct microbial communities in the gastrointestinal tracts of goats. **A** Alpha diversity indexes of ASV profiles based on DNA- and RNA-level 16S rRNA analysis. **B** Comparison of overall community between two fiber types in three GIT regions based on bray curtis distances of ASV profiles in DNA- and RNA-level 16S rRNA analysis, respectively. **C** Principal coordinate analysis (PCoA) of microbial community between two fiber types in each GIT region. **D** Relative abundances of the top 30 genera in response to dietary fiber types. R_FF, rumen in fast-fermentation fiber; R_SF, rumen in slow-fermentation fiber; I_FF, ileum in fast-fermentation fiber; I_SF, ileum in slow-fermentation fiber; C_FF, cecum in fast-fermentation fiber; C_SF, cecum in slow-fermentation fiber. The asterisks denote significant P values, $*P < 0.05$; $**P < 0.01$

Thereafter, we focused on the carbohydrate metabolic cascades of microorganisms in response to different dietary fiber types in the entire GIT of goats. The overall CAZyme profile of GIT microbiome was remarkably affected by fiber types in the rumen and cecum ($P < 0.05$, Fig. 3C). Concretely, the SF diet selected for greater abundances of cellulolytic enzyme (GH3), and hemicellulolytic enzymes (GH10, GH43, and GH51) in the rumen, phylogenetically assigned to *Prevotella*, *Butyrivibrio*, and *Fibrobacter* ($P < 0.05$, Fig. 3D and Fig. S4). In the cecum, the SF diet selected for greater abundances of hemicellulolytic enzyme GH10, which were mainly assigned to *Bacteroides* and *Ruminococcus* at the genus level (Fig. 3D). Interestingly, abundances of pectinases, including PL1, GH28, and CE8, were greater with FF diets in the rumen and cecum ($P < 0.05$, Fig. 3D). These pectinases were mainly assigned to *Prevotella* and *Bacteroides* in the rumen, and *Bacteroides* and *Clostridium* in the cecum (Fig. 3D). These results derived from gene abundance profiles revealed that the FF treatment promoted pectin degradation, whereas the SF diet selected depolymerization of cellulose and hemicellulose in the rumen and cecum.

Pentose or hexose produced from depolymerization of cellulose, hemicellulose, and pectin were used as substrates to generate pyruvate via the glycolysis pathway, which was further fermented into acetate, propionate, and butyrate by GIT microbiome. Of note, the SF diet selected for a greater abundance of genes involved in the glycolysis pathway in the rumen and ileum ($P < 0.05$, Fig. 3E, Fig. S5, and Table S4). As anticipated, genes involved in SCFA biosynthesis were remarkably affected by dietary fiber types in a GIT region-specific pattern. In the rumen, the SF diet selected for a greater abundance of genes involved in acetyl-CoA/lactate to acetate production (AAP/LAP, including *pta*, *acsA*, and *ackA*) and succinate to propionate production pathways (SPP, including *sdhA*, *sdhB*, and *fumB*) ($P < 0.05$, Fig. 3F, Fig. S6). In contrast, the SF cecal microbiome encoded a greater proportion of enzymes that produce butyrate (ABP, including *paaH* and *ACAT*). Notably, these SCFA biosynthesis enzymes were mainly assigned to *Prevotella*, *Bacteroides*, and *Butyrivibrio* in the rumen, while classified as

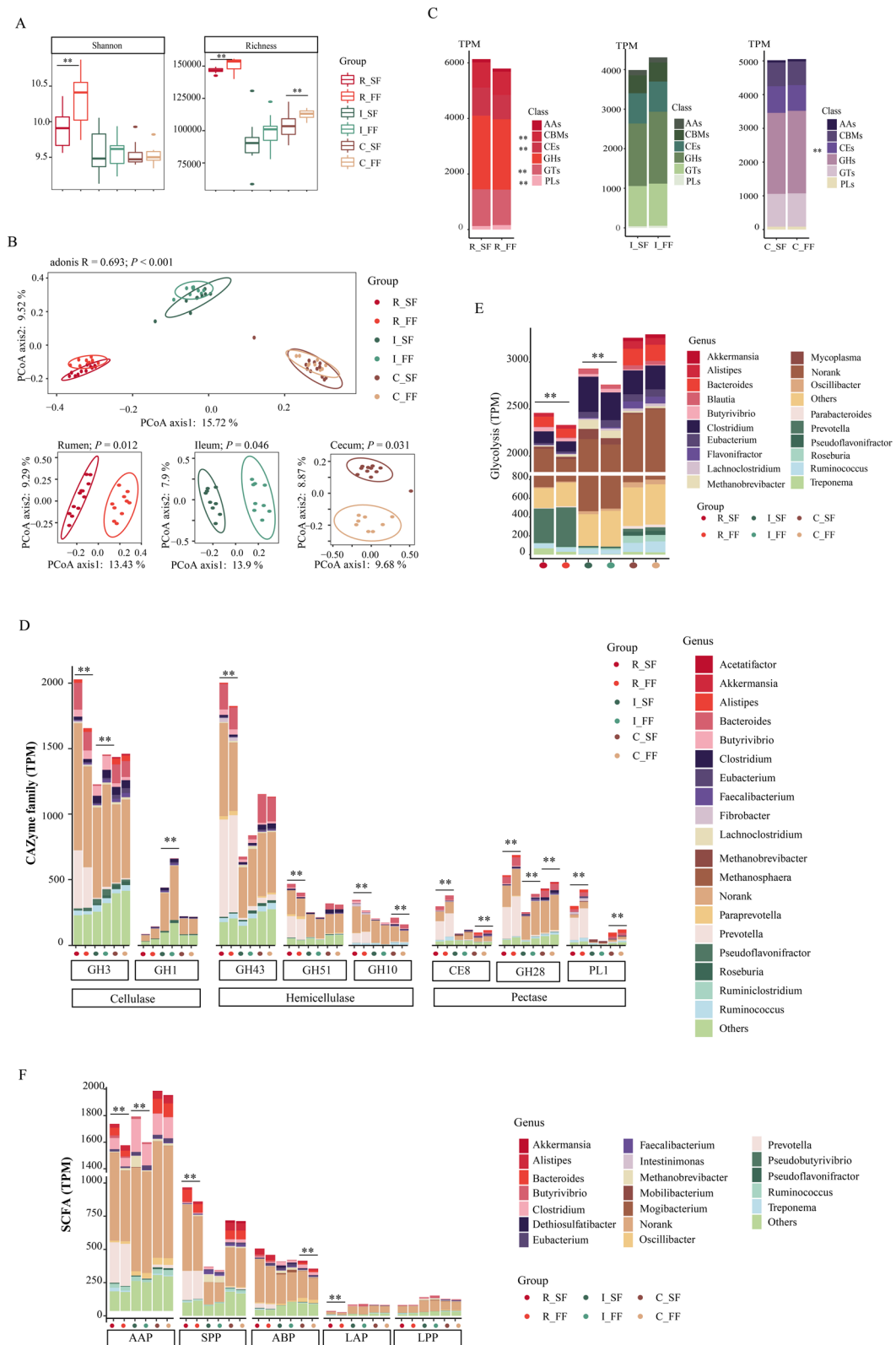
Ruminococcus, *Clostridium*, and *Butyrivibrio* spp. in the cecum (Fig. 3F). These results, along with the measured SCFA profiles at the metabolic level, indicated that SF diet enhanced fiber depolymerization to produce acetate in the rumen, while the unfermented fiber flowed to the cecum to produce more butyrate.

Microbial mediated metabolism of energy impacted by dietary fiber types

The majority of ATP, the energy currency of life in microbes, is produced through two major mechanisms: substrate-level phosphorylation (SLP) and electron transport phosphorylation (ETP) [41]. Under anaerobic conditions, most microbial fermentations produce ATP primarily by SLP, which facilitates ATP synthesis through glycolysis, where the high-energy phosphate groups are directly transferred from the substrate molecule to ADP [42]. Meanwhile, ETP utilizes the electrochemical potential generated by the respiratory chain to drive efficient ATP synthesis via the ATP synthases, also called ATPases [43]. Herein, we identified 7 microbial genes contributing to SLP enzymes and 34 microbial genes encoding ATPases, comprising of F-type, V/A-type, and V-type synthases (Table S5). Despite alpha diversity being similar in two treatments ($P > 0.05$, Fig. 4A), dietary fiber types selected distinct microbial-mediated energy metabolism in the rumen ($P < 0.05$, Fig. 4B). In terms of SLP enzymes, SF treatment selected for a greater abundance of genes involved in glycolysis (phosphoglycerate kinase, *PGK*) and acetate production (acetate kinase, *ackA*), while a lower abundance of genes involved in succinate production (succinyl-CoA synthetases, *sucC* and *sucD*) in the rumen ($P < 0.05$, Fig. 4C and D). Despite the abundances of V-type ATPases were quite low with a TPM value of < 4 , SF treatment selected for a greater abundance of key genes involved in both F-type (*ATPF1A*, *ATPF1B*, and *ATPF0B*) and V/A-type (*ATPV1* and *ATPVE*) ATPases in the rumen ($P < 0.05$, Fig. 4C and D), while there were no significant differences between two treatments in the ileum and cecum ($P > 0.05$). Phylogenetic origin of the dominant SLP enzymes and F-type ATPases showed that they were mainly assigned to *Prevotella* and *Bacteroides* in the rumen (Fig. 4E). In addition, the abundance of SLP

(See figure on next page.)

Fig. 3 Fast- and slow-fermentation fiber treatments exhibit distinct gene profiles of CAZymes and KEGG enzymes implicated in fiber degradation process in the GIT microbiome of goats. **A** Shannon and richness indexes of carbohydrate-related genes. **B** PCoA profile of carbohydrate-related genes between two fiber types in all GIT regions (top) and individual GIT region (bottom). **C** CAZyme abundance at class level. **D** CAZyme family distributions assigned by genus. **E** Glycolysis-related gene distributions assigned by genus. **F** SCFA production gene distributions assigned by genus. R_FF, rumen in fast-fermentation fiber; R_SF, rumen in slow-fermentation fiber; I_FF, ileum in fast-fermentation fiber; I_SF, ileum in slow-fermentation fiber; C_FF, cecum in fast-fermentation fiber; C_SF, cecum in slow-fermentation fiber. AAP, acetyl-CoA to acetate production; SPP, succinate to propionate production; ABP, acetyl-CoA to butyrate production; LAP, lactate to acetate production; LPP, lactate to propionate production. The asterisks denote significant P values, * $P < 0.05$; ** $P < 0.01$



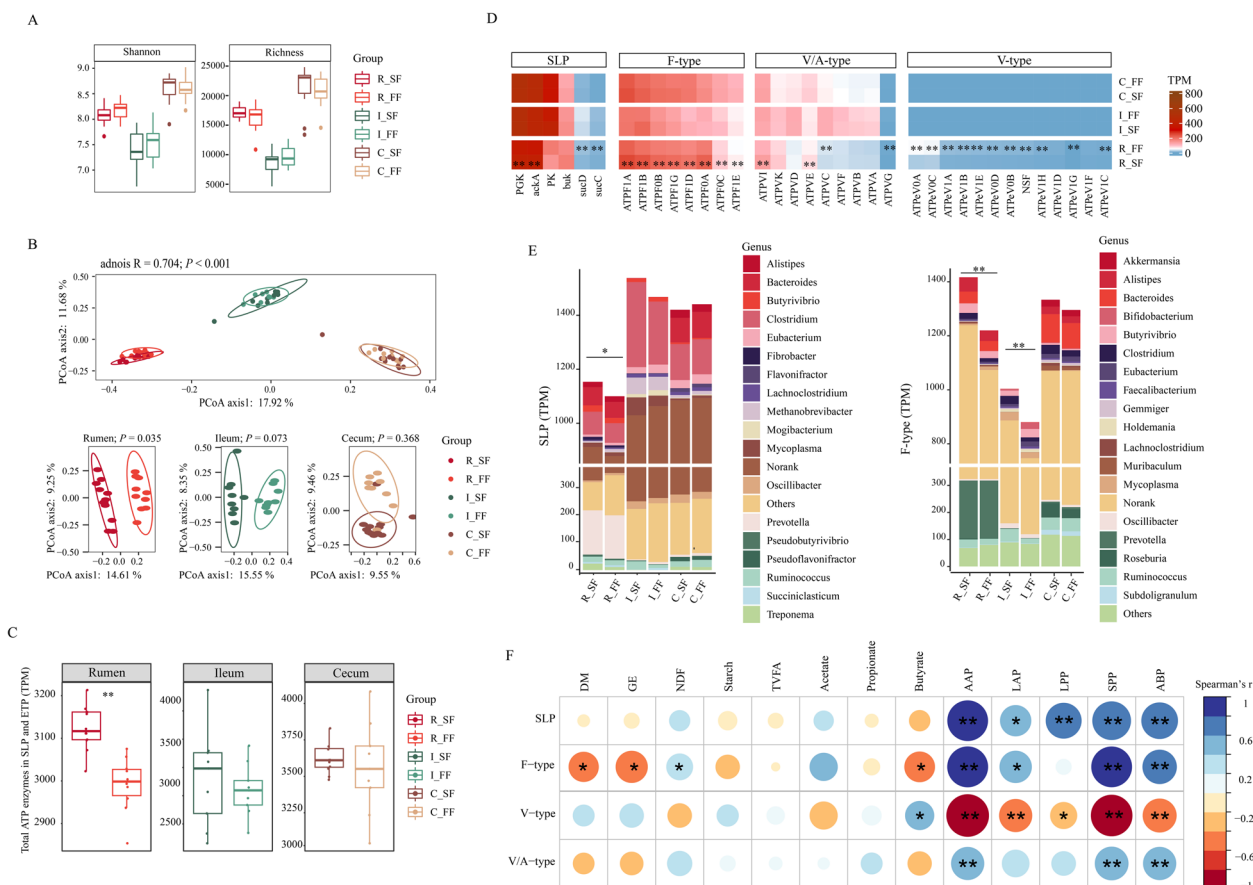


Fig. 4 Fast- and slow-fermentation fiber treatments alter the abundances of substrate-level phosphorylation (SLP) enzymes and ATPases in the GIT microbiome of goats. **A** Shannon and richness indexes of genes encoding SLP enzymes and ATPases. **B** PCoA profile of genes encoding SLP enzymes and ATPases between two fiber types in all GIT regions (top) and individual GIT region (bottom). **C** Boxplot of total abundance of SLP enzymes and ATPases. **D** Heatmap of abundance of SLP enzymes and F-type, V/A-type, and V-type ATPases. **E** SLP enzymes (left) and F-type ATPase (right) gene distributions assigned by genus. **F** Correlation between the abundance of genes involved in ATP production, and nutrient digestibility, SCFA profile, abundance of genes involved in SCFA biosynthesis. R_FF, rumen in fast-fermentation fiber; R_SF, rumen in slow-fermentation fiber; I_FF, ileum in fast-fermentation fiber; I_SF, ileum in slow-fermentation fiber; C_FF, cecum in fast-fermentation fiber; C_SF, cecum in slow-fermentation fiber. The asterisks denote significant P values, * $P < 0.05$; ** $P < 0.01$

enzymes and F-type ATPases were positively correlated with NDF digestibility and ruminal acetate production (Fig. 4F). Thus, SF diet enhanced energy generating and consuming to promote fiber utilization by altering distinct microbial SLP enzymes and ATPases in the rumen.

Microbial mediated biosynthesis of cobalamin in response to fiber types

Considering the indispensability of cobalamin as a cofactor in carbon and energy metabolism, as well as “cofactors and vitamins” pathway was affected by dietary fiber types as mentioned above, microbial genes involved in cobalamin biosynthesis were screened to clarify responses to different fiber types throughout the entire GIT. We identified 68 KEGG orthologues (KOs) involved in microbial mediated cobalamin biosynthesis, comprising of sequential action of precorrin- 2 synthesis pathway,

aerobic or anaerobic pathway, post-adochi-P pathway, and salvage pathway (Table S6, Fig. S7). Alpha diversity as measured by Richness and Shannon indexes were greater for the FF treatment when compared to those in the SF treatment in the ileum ($P < 0.05$, Fig. 5A), whereas the alpha diversity indices were similar in both treatments in the rumen and cecum. Meanwhile, dietary fiber types selected distinct microbial-mediated cobalamin biosynthesis potentials in the rumen, ileum, and cecum ($P < 0.05$, Fig. 5B). Particularly, SF treatment enriched for precorrin- 2 synthesis pathway (hemD, gltX); aerobic pathway (cbiT, cobD); anerobic pathway (cobS-co, cob); and post-adochi-P pathway (cobT- α , cobU-ade) in the rumen ($P < 0.05$, Fig. 5C and D). Analogously, abundance of genes involved in anaerobic (cbiG) and aerobic (cobL and cobH) pathways were enriched by SF treatment in the ileum ($P < 0.05$), whereas only *cysG* gene was

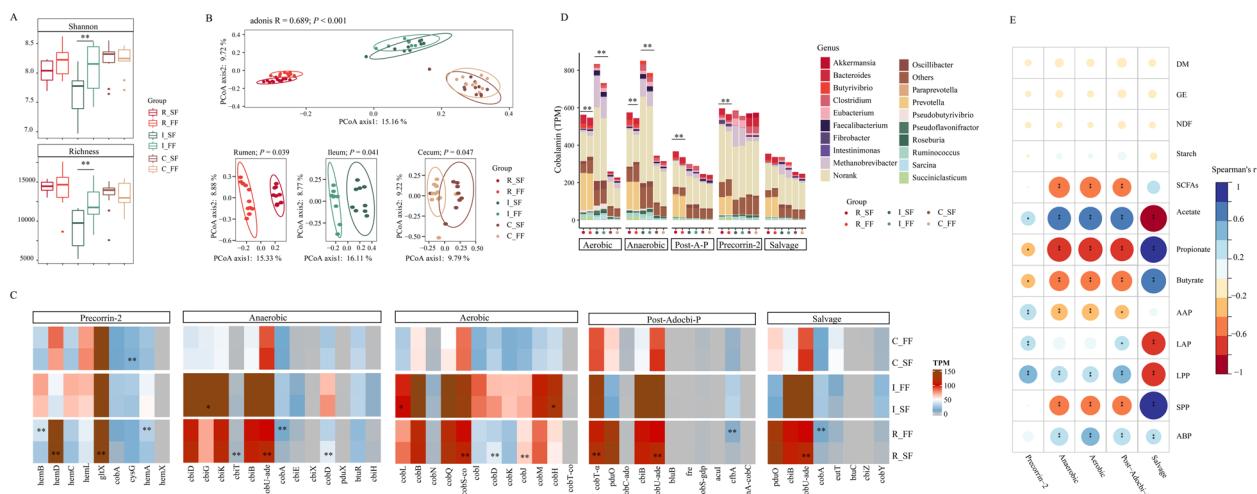


Fig. 5 Fast- and slow-fermentation fiber treatments result in distinct cobalamin biosynthesis gene levels in the GIT microbiome of goats. **A** Shannon and richness indexes of genes related to cobalamin biosynthesis. **B** PCoA profile of genes involved in cobalamin biosynthesis between two fiber types in all GIT regions (top) and individual GIT region (bottom). **C** Heatmap of abundances of kos related to cobalamin biosynthesis. **D** Cobalamin biosynthesis gene distributions assigned by genus. **E** Correlation between the abundance of cobalamin biosynthesis genes and nutrient digestibility, SCFA profile, abundance of genes involved in SCFA biosynthesis. R_FF, rumen in fast-fermentation fiber; R_SF, rumen in slow-fermentation fiber; I_FF, ileum in fast-fermentation fiber; I_SF, ileum in slow-fermentation fiber; C_FF, cecum in fast-fermentation fiber; C_SF, cecum in slow-fermentation fiber. The asterisks denote significant *P* values, **P* < 0.05; ***P* < 0.01

increased by SF treatment in the cecum (*P* < 0.05). Phylogenetic origin of cobalamin biosynthetic genes showed that they were mainly assigned to *Prevotella*, *Bacteroides*, and *Butyrivibrio* in the rumen, while classified as *Methanobrevibacter* and *Oscillibacter* in the ileum, as well as *Ruminococcaceae*, *Akkermansia*, and *Clostridium* in the cecum (Fig. 5D). Correlation analysis emphasized the involvement of cobalamin biosynthesis in acetate production, particularly in the corrinoid protein methylation and acetyl-CoA assembly steps (Fig. 5E). Those indicated the possibility that the diet with SF may have greater potential capacity of cobalamin biosynthesis due to the distinct microbial activities.

Functional microbial taxa capable of fiber degradation were differentially abundant in FF and SF GIT microbiome

To resolve the functional relationships among GIT microbiota in carbohydrate metabolism, we co-assembled and binned all metagenomes, yielding 1029 non-redundant high-quality MAGs spanning 120 bacterial and 11 archaeal classes (Fig. 6A, Table S7). As anticipated, over 80% genomes were affiliated with the dominant GIT class *Clostridia* (524 MAGs) and *Bacteroidia* (311 MAGs), including 27.0% *Prevotella* (57 MAGs) and 8.8% *Ruminococcus* (46 MAGs) (Fig. 6A). Further insights into key metabolic genes indicated that 813, 460, 738, and 140 MAGs were predicted to possess the capability to depolymerize fiber, produce SCFAs, generate ATP, and biosynthesize cobalamin, respectively (Fig. 6B). Notably,

MAG530 (CAG- 791 spp.) and MAG514 (UBA1066 spp.) encoded key metabolic genes involved in all the above four processes, demonstrating a close link between cobalamin biosynthesis and fiber degradation processes in GIT microbiome.

Then, we investigated the relative abundance of the assembled genomes in response to the intervention of fiber types in individual GIT sections (Table S8, Fig. S8). In the rumen, 136 and 145 functional MAGs were more enriched in SF and FF samples respectively (Fig. 6C, D). Specifically, two MAGs affiliated to *Fibrobacter* spp. (MAG686, MAG768), three MAGs classified as *Ruminococcus* spp. (MAG697, MAG914, and MAG989), representative cellulolytic bacteria, were substantially enriched in the SF treatment (*P* < 0.01, over fourfold greater). Three MAGs affiliated to *Saccharofermentans* spp. (MAG554, MAG577, and MAG763), putative acetogenic bacteria, also experienced an enrichment with > 15-fold increase in the SF treatment (*P* < 0.01). Meanwhile, MAG621 (*Ruminococcus* spp.), MAG643 (*Eubacterium* spp.), MAG383 (UBA2862 spp.), and MAG753 (UBA1774 spp.), which harbor most of genes involved in vitamin B₁₂ biosynthesis and referred as potential cobalamin producers (Table S9), were considerably enriched (*P* < 0.01, over threefold greater) in SF goats. Conversely, the rumen of FF goats selected pectin-degrading *Prevotella* spp. (MAG735 and MAG782; *P* < 0.01, 25.5- and 29.9-fold greater), and putative butyrate-producing RUG099 spp. (MAG512, MAG518, and MAG538; *P* < 0.01, over threefold greater).



Fig. 6 Functional microbial taxa capable of fiber degradation are differentially abundant in the GIT microbiome of FF and SF goats. **A** Phylogenetic tree of 1029 metagenome-assembled genomes (MAGs). The outer strip chart indicates the class-level affiliations of MAGs, and the height of the outermost bar represents the genome size. **B** Correlation network of metabolic pathways and genomes, with genomes colored according to taxonomic information; Heatmap for selected key CAZyme families in differentially enriched genomes in SF or FF ruminal microbiome (**C**) and SF or FF cecal microbiome (**E**); Heatmap for selected key metabolic genes in differentially enriched genomes in SF or FF ruminal microbiome (**D**) and SF or FF cecal microbiome (**F**), key metabolic genes include SCFA production, energy generating and cobalamin biosynthesis

Analogously, 105 MAGs and 148 MAGs were preferentially enriched in the cecum of FF and SF goats, respectively (Fig. 6E, F). Intriguingly, potential cellulolytic *Fibrobacter* spp. (MAG358, MAG686, and MAG759) and *Bacteroides* spp. (MAG043) were consistently enriched in the SF treatment ($P < 0.01$, 176.8-, 6.1-, 7.4- and 14.6-fold greater), and this was accompanied by the enrichment

of the butyrate-producing *Butyrivibrio* spp. (MAG999) with 5.0-fold increase ($P < 0.01$). Whereas, the cecum of FF goats selected speculatively pectin-degrading *Alis-tipes* spp. (MAG210, MAG398, over sevenfold greater) and acetate-producing UBA2862 spp. (MAG309, 8.9-fold greater). These results further upheld that the FF diet selectively enriched potential pectin degraders to

enhance animal growth, while the SF diet stimulated fibrolytic bacteria to improve fiber utilization in a GIT region dependent manner (Fig. 7).

Discussion

As a diverse group of non-digestible carbohydrates that differ in structural components, physicochemical characteristics, and physiological effects, dietary fibers play a vital role in maintaining the productivity and health of animals [44, 45]. Herein, a goat model of FF and SF diet was developed to depict characteristic microbiome and metabolic strategies to different fiber polysaccharides in separate GIT regions. Intriguingly, SF and FF goats exhibited different performance phenotypes, as featured by greater fiber digestibility and weight gain, respectively. It is well recognized that the soluble (pectin, β -glucan, and galactomannan) and insoluble (cellulose, hemicellulose, and lignin) fiber fractions of the plant cell walls could determine its fermentability and subsequent functionality in the GIT [44]. Obviously, our data suggest that the key metabolic pathways and underlying mechanisms

through which dietary fiber benefits the host animals are likely fiber types dependent, mainly attributed to variation in the fiber content and polysaccharide chemistry (cellulose, hemicellulose, and pectin).

Increasing evidence highlights the significance of the GIT microbiota as a central actor in driving dietary fiber beneficial effects in humans and animals, with SCFAs as key bacterial metabolites [46]. The special rumen microorganisms elaborate a variety of enzyme combinations for fiber degradation and are the pioneers of top priority to break down plant carbohydrates [4]. In this study, we focused on the prokaryotic community, due to the low metagenomic sequence numbers and analytical method limitation of eukaryotic community, including protozoa and anaerobic fungi [47, 48]. In Holstein heifers, ruminal pH could regulate fiber degradation and fermentation by shifting the microbial community and gene expression of carbohydrate-active enzymes [49]. Moreover, there has been speculation that the fiber-rich diet selected for ruminal fibrolytic bacteria and resulted in elevated fiber utilization in cattle [13]. Likewise, the SF

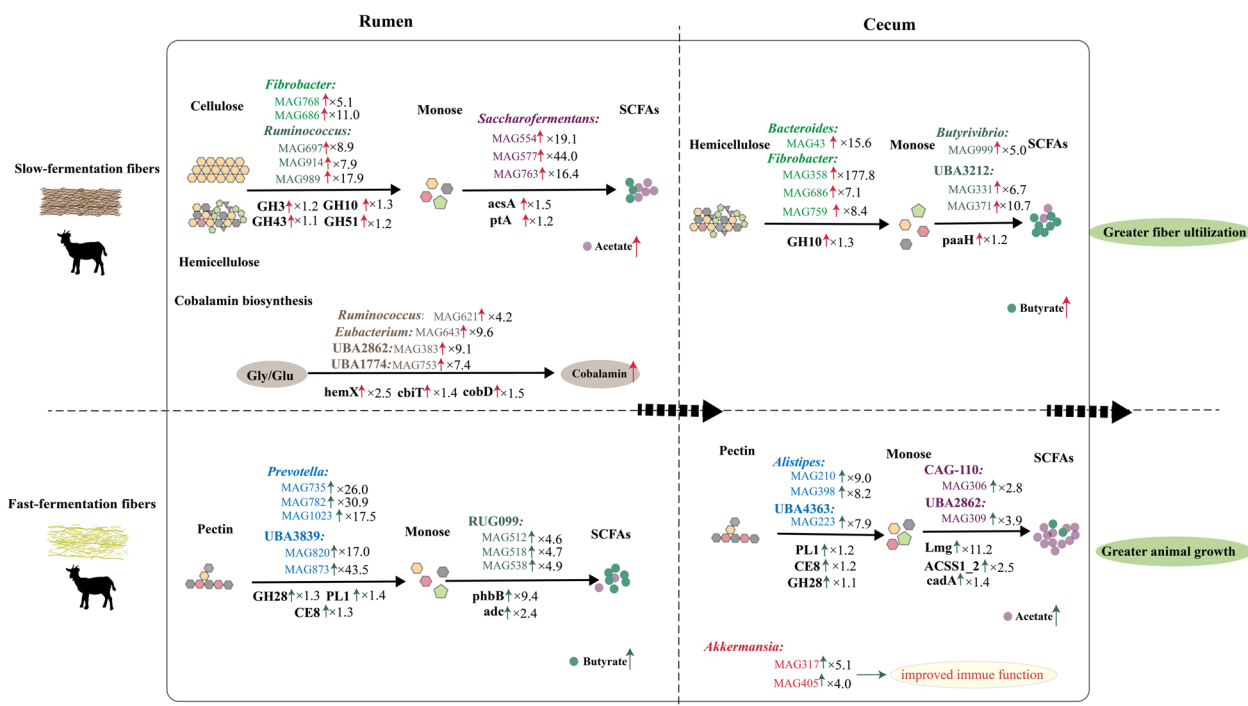


Fig. 7 Fast- and slow-fermentation fiber treatments exhibit distinct microbial fiber utilization pathways in the rumen and cecum of goats. Top, SF diet selected fiber-degrading bacteria to enhance cellulose and hemicellulose depolymerization, which is closely related to microbial cobalamin biosynthesis process. The resulting monosaccharides were utilized by acetogens to produce more acetate in the rumen (left). Unfermented fiber flowed to the cecum, where it encountered additional degradation by fiber-degrading bacteria, and produced more butyrate by butyrate-producing bacteria (right). These SF selected microbial utilization processes of cellulose and hemicellulose contributed to greater fiber utilization. Bottom, FF diet selected pectin-degrading bacteria and butyrate-producing bacteria to produce more butyrate in the rumen (left). Pectin was further degraded in the cecum and resulted in more acetate production (right). These FF selected microbial utilization processes of pectin was more favorable for animal growth. The fold changes (red arrows, SF/FF; green arrows, FF/SF) of enzymes or MAGs in each group are labeled besides, and presented in Table S8 in details

diet preferentially selected for fibrolytic microorganisms *Fibrobacter* and *Ruminococcus*, and enriched for genes encoding for 1,4-beta-xylosidase (GH3), and endoglucanase (GH8 and GH9) in the rumen. The SF diet with greater NDF, cellulose, and hemicellulose represents poor-quality forage diet, and proliferation of fibrolytic bacteria has been proposed as a crucial energy harvesting strategy for ruminants to adapt to harsh dietary and environmental conditions [13, 50, 51]. Furthermore, enrichment of potentially acetogenic members *Saccharofermentans* spp. and increased abundance of acetyl-CoA synthase (*acs*) gene contribute to the greater ruminal acetate production [46]. On the contrary, the rapid generation of SCFAs in the rumen from FF diet may be driven by its greater pectin fraction, which has previously been shown to be fermented at a rate greater than cellulose and hemicellulose [52, 53]. Pectin develops an extremely complex structure in terms of monosaccharide composition, glycosidic linkage types, and non-glycosidic substituents and is primarily comprised of homogalacturonan, Rhamnogalacturonan I, and Rhamnogalacturonan II. As such, its degradation is mediated by a wide range of enzymes for the depolymerization of pectin backbone, and the removal of accessory side chains [54]. As anticipated, several potential pectin degraders, *Prevotella* spp. and UBA3839 spp. experienced a surge in response to the FF diet, along with the increased abundance of pectinolytic genes encoding for polygalacturonase (GH28), pectate lyase (PL1), and CE8 (pectin methylesterase). Afterwards, the resulting monosaccharide was degraded by putative butyrate-producing bacteria RUG099 spp. (MAG512 and MAG538). Genomic analysis confirms their ability to produce pyruvate from lactate (*ldh*), and condensation of acetyl CoA with subsequent reduction to butyryl CoA (*buk*) results in the formation of butyrate in the rumen of FF goats [46, 55].

Notably, this study emphasizes the importance of hindgut microbiome in fiber digestion process in vivo, which substantiates our previous in vitro incubation study [15]. The SF diet selected fibrolytic bacteria (*Fibrobacter* and *Bacteroides*) and enriched for genes encoding for endoxylanase (GH10). Previous studies indicated that microbial fermentation in the hindgut complements rumen digestion, accounting for digestion of 18 to 27% and 30 to 40% of the total cellulose and hemicellulose digested per day, respectively [56]. Insights from SCFA production indicate that SF diet favored butyrate production in the cecum at both gene and metabolic levels. This disparity in SCFA production pattern by the rumen and hindgut microorganisms might be explained by two reasons. Firstly, the foregut and hindgut of ruminants exhibited profound discrepancies in the resident microbes and their substrate availability [57, 58]. Secondly, the cecal

SCFA concentrations measured in this study represent the net result of their production and absorption, and more than 90% of the SCFAs are actively absorbed and metabolized by the hindgut epithelial cells in nonruminants [44]. Another notable phenomenon lies in the increase of *Akkermansia* spp. in the cecum of FF goats. As a typically recognized mucin-degrading bacterium, its increase will be linked to the improved immune function, and thereafter elicits greater animal growth in the FF goats [59]. Further studies are warranted to determine the orchestrated host-microbiota interplay in terms of SCFA fate in the entire GIT, and thereafter which fiber sources, which physicochemical characteristics, and how they achieve optimal growth and health benefits of ruminants.

Generally, most anaerobic microbial fermentations produce ATP primarily by substrate-level phosphorylation (SLP) [60]. In this study, the abundances of SLP enzymes, in particular phosphoglycerate kinase (PGK) in glycolysis and acetate kinase (*ackA*) in acetate production, were significantly increased in the rumen with the shift to the SF diet. This might be due to the fact the SF diet promoted the microbial fermentation into acetate production, which predominantly involved glycolysis [4, 42]. On the other hand, energy can be also interconverted with the transfer of protons or sodium cations across membranes with ATP hydrolysis or synthesis, referred to as electron transport phosphorylation (ETP) [61]. Three rotary ATPases are responsible for this fundamental energy conversion, which are reversible protein complexes comprising of eukaryotic vacuolar H⁺-ATPases (V-ATPase), bacterial or archaeal V/A ATPases, and F-type F₀F₁ ATPases [62]. Intriguingly, V/A ATPases exhibited in low abundance in GIT microorganisms of goats and were phylogenetically from eukaryotic consortia including ciliate (Ciliophora phylum) and fungi (Ascomycota phylum), confirming the prominence of prokaryotes implicated in energy homeostasis [4]. Particularly, SF treatment enhanced energy generating and consuming dynamics in the rumen to promote fiber utilization, as characterized by greater abundances of key SLP enzymes and F-type ATPases. These microbial ATPase-based enzymatic apparatuses provide an avenue forward to unveil the possible energy harvest strategy for the conversion of these low-quality plant fibers into value-added products in ruminants.

As a micronutrient of essential importance to amino acid synthesis, energy metabolism, DNA replication and repair, cobalamin can influence primary productivity, community dynamics and ecological interactions in GIT microbial consortia [63]. Consistent with previous culture- and omics-based study [19, 64], this study found that potential cobalamin producers comprise a restricted

set the GIT microbial consortia, including *Ruminococcus* spp., *Eubacterium* spp., and UBA2862 spp. Moreover, the SF diet favored microbial cobalamin biosynthesis in the rumen, as featured by considerable enrichment of de novo biosynthetic genes. Likewise, cobalamin biosynthetic capacity was enhanced when dietary roughage level was increased to 60% from 40% in dairy cows [19]. Collectively, it is plausible to infer that dietary fiber types (fiber content and polysaccharide chemistry) are of importance for the intricate and costly cobalamin biosynthesis process.

Conclusions

In summary, microbial utilization dynamics of dietary fibers are governed by fiber types (fiber content and polysaccharide chemistry) in a GIT region dependent manner in goats. Slow-fermentation fiber selects fibrolytic bacteria in the rumen and cecum to enhance cellulose and hemicellulose degradation, which might be mediated by microbial B₁₂ biosynthesis process. Fast-fermentation fiber favors pectin-degrading bacteria and pathways to improve animal growth (Fig. 7). The subsequent SCFA patterns and metabolic pathways unveil distinctive energy harvest strategies during degradation of different fiber polysaccharides for the rumen and hindgut microbes, and appeal for future microbial-related research endeavors from the whole gastrointestinal perspective. Further study applying single-cell microbial sequencing and enrichment analysis is also warranted to depict the vital role of the eukaryotic community in fiber digestion.

Supplementary Information

The online version contains supplementary material available at <https://doi.org/10.1186/s40168-025-02112-y>.

Additional file 1: Table S1. Composition and nutrient levels of two diets (DM basis). Table S2. Experiment design of 61 metagenomic samples in this study. Table S3. Summary of metagenomic sequence data generated from 61 GIT samples. Table S4. List of genes and kos involved in glycolysis and SCFA production. Table S5. List of genes and kos involved in ATP production. Table S6. List of genes and kos involved in vitamin B₁₂ biosynthesis. Table S7. Taxonomy of 1029 assembled MAGs in this study. Table S8. DESeq2 results of MAGs between SF vs. FF diets in each GIT. Table S9. Gene information of 1029 metagenome-assembled genomes, including fiber digestion, SCFA production, ATPase, and vitamin B₁₂ biosynthesis. Fig. S1. Differential microbial taxa between fast- and slow-fermentation fiber diets of goat at species level in the rumen (A), ileum (B) and cecum (C) based on the metagenomic data using kraken2. The x-axis displays the corrected *p*-value, and point size displays the fold changes. Red points display greater abundance in FF treatment, white blue points display greater abundance in SF treatment. Fig. S2. Correlation between differential microbial genera at DNA- (A) or RNA- level (B), and phenotypes including nutrient digestibility and fermentation parameters. Red and blue colors represent negative and positive correlations, respectively. Asterisks denote Spearman's significance levels. **P* < 0.05, ***P* < 0.01. Fig. S3. Changes in KEGG level 1 (A) and level 2 (B) pathways in response to dietary fiber types in the GIT of goats. R_FF, rumen in fast-fermentation fiber; R_SF, rumen in slow-fermentation fiber; I_FF, ileum in fast-fermentation fiber; I_SF, ileum in slow-fermentation fiber; C_FF, cecum in fast-fermentation fiber; C_SF, cecum in slow-fermentation fiber. Fig. S4. Heatmap of abundances of

microbial CAZymes involved in cellulose, hemicellulose and pectin depolymerization in the GIT of goats. R_FF, rumen in fast-fermentation fiber; R_SF, rumen in slow-fermentation fiber; I_FF, ileum in fast-fermentation fiber; I_SF, ileum in slow-fermentation fiber; C_FF, cecum in fast-fermentation fiber; C_SF, cecum in slow-fermentation fiber. Fig. S5. Heatmap of abundances of microbial genes involved in glycolysis pathway in the GIT of goats. Asterisks denote significant *p* values: **P* < 0.05, ***P* < 0.01. R_FF, rumen in fast-fermentation fiber; R_SF, rumen in slow-fermentation fiber; I_FF, ileum in fast-fermentation fiber; I_SF, ileum in slow-fermentation fiber; C_FF, cecum in fast-fermentation fiber; C_SF, cecum in slow-fermentation fiber. Fig. S6. Heatmap of abundances of microbial genes involved in SCFA production in the GIT of goats. Asterisks denote significant *p* values: **P* < 0.05, ***P* < 0.01. R_FF, rumen in fast-fermentation fiber; R_SF, rumen in slow-fermentation fiber; I_FF, ileum in fast-fermentation fiber; I_SF, ileum in slow-fermentation fiber; C_FF, cecum in fast-fermentation fiber; C_SF, cecum in slow-fermentation fiber. Fig. S7. The pathway of cobalamin *de novo* biosynthesis. Fig. S8. The differential MAGs between fast- and slow-fermentation fiber diets of goat in the rumen (A), ileum (B) and cecum (C). The x-axis displays the corrected *p*-value, and point size displays the fold changes. Red points display greater abundance in FF treatment, and blue points display greater abundance in SF treatment.

Acknowledgements

Not applicable.

Authors' contributions

X.Z., J.W., and J.J. collected and analyzed the data. X.Z. and J.J. wrote the manuscript. J.J., R.Z., and Z.T. conceived and designed the study. All authors have read and approved the final manuscript.

Funding

This work was supported by the National Natural Science Foundation of China (32372829, 31972992), Hunan Provincial Natural Science Foundation of China (2023JJ10047), The Science and Technology innovation Program of Hunan Province (2022RC1158), and Youth Innovation Promotion Association CAS (2023382).

Data availability

Raw sequence reads for all samples have been deposited into the China National GeneBank DataBase (CNGBdb) with accession number CNP0004995.

Declarations

Ethics approval and consent to participate

All experimental animals were used in accordance with the Animal Care Committee, Institute of Subtropical Agriculture, Chinese Academy of Science, Changsha, China (Approval No: ISA-R-2020-16).

Consent for publication

Not applicable.

Competing interests

The authors declare no competing interests.

Received: 30 July 2024 Accepted: 11 April 2025

Published online: 11 May 2025

References

- Food and Agriculture Organization of the United Nations (FAO). Land use. In: FAOSTAT. 2025. <https://www.fao.org/faostat/en/#data/RL>.
- FAO, IFAD, UNICEF, WFP and WHO. In Brief to The State of Food Security and Nutrition in the World 2024—financing to end hunger, food insecurity and malnutrition in all its forms. 2024; Rome. <https://doi.org/10.4060/cd1276en>.
- Zhang X, Wu J, Zhou C et al. Temporal changes in muscle characteristics during growth in the goat. *Meat Sci.* 2023;109145.

4. Mizrahi I, Wallace RJ, Morais S. The rumen microbiome: balancing food security and environmental impacts. *Nat Rev Microbiol*. 2021;19:553–66.
5. Li F, Hitch TCA, Chen Y, et al. Comparative metagenomic and metatranscriptomic analyses reveal the breed effect on the rumen microbiome and its associations with feed efficiency in beef cattle. *Microbiome*. 2019;7:6.
6. Flint HJ, Bayer EA, Rincon MT, et al. Polysaccharide utilization by gut bacteria: potential for new insights from genomic analysis. *Nat Rev Microbiol*. 2008;6:121–31.
7. Vahmani P, Ponnampalam EN, Kraft J, et al. Bioactivity and health effects of ruminant meat lipids. *Invited Review Meat Sci*. 2020;165:108114.
8. Rahimi J, Fillol E, Mutua JY, et al. A shift from cattle to camel and goat farming can sustain milk production with lower inputs and emissions in north sub-Saharan Africa's drylands. *Nat Food*. 2022;3:523–31.
9. Jiao JZ, Huang JY, Zhou CS, et al. Taxonomic identification of ruminal epithelial bacterial diversity during rumen development in goats. *Appl Environ Microbiol*. 2015;81:3502–9.
10. Cabral L, Persinoti GF, Paixao DAA, et al. Gut microbiome of the largest living rodent harbors unprecedented enzymatic systems to degrade plant polysaccharides. *Nat Commun*. 2022;13:629.
11. Calusinska M, Marynowska M, Bertucci M, et al. Integrative omics analysis of the termite gut system adaptation to *Miscanthus* diet identifies lignocellulose degradation enzymes. *Commun Biol*. 2020;3:275.
12. Greening C, Geier R, Wang C, et al. Diverse hydrogen production and consumption pathways influence methane production in ruminants. *ISME J*. 2019;13:2617–32.
13. Li QS, Wang R, Ma ZY, et al. Dietary selection of metabolically distinct microorganisms drives hydrogen metabolism in ruminants. *ISME J*. 2022;16:2535–46.
14. Godoy-Vitorino F, Goldfarb KC, Karaoz U, et al. Comparative analyses of foregut and hindgut bacterial communities in hoatzins and cows. *ISME J*. 2012;6:11.
15. Jiao JZ, Wang PP, He ZX, et al. In vitro evaluation on neutral detergent fiber and cellulose digestion by post-ruminal microorganisms in goats. *J Sci Food Agr*. 2014;94:1745–52.
16. Deniz A, Aksoy K. Use of organic phosphorous butafosfan and vitamin B12 combination in transition dairy cows. *Veterinárni medicína*. 2022;67:334–53.
17. Duplessis M, Lapiere H, Girard CL. Biotin, folic acid, and vitamin B12 supplementation given in early lactation to Holstein dairy cows: their effects on whole-body propionate, glucose, and protein metabolism. *Anim Feed Sci Tech*. 2022;292:292.
18. Zhou J, Yu X, Liu J, et al. VB12Path for accurate metagenomic profiling of microbially driven cobalamin synthesis pathways. *mSystems*. 2021;6:16.
19. Jiang Q, Lin L, Xie F, et al. Metagenomic insights into the microbe-mediated B and K(2) vitamin biosynthesis in the gastrointestinal microbiome of ruminants. *Microbiome*. 2022;10:109.
20. Smith DP. Effect of quartering and sampling method on recovery of bacteria from broiler carcasses. *Poult Sci*. 2008;87:40–1.
21. Jiao J, Zhou C, Guan LL, et al. Shifts in host mucosal innate immune function are associated with ruminal microbial succession in supplemental feeding and grazing goats at different ages. *Front Microbiol*. 2017;8: 1655.
22. Zhang X, Li X, Wu J, et al. Rumen-protected glucose supplementation in transition dairy cows shifts fermentation patterns and enhances mucosal immunity. *Anim Nutr*. 2021;7:1182–8.
23. Tian C, Wu J, Jiao J, et al. Short communication: a high-grain diet entails alteration in nutrient chemosensing of the rumen epithelium in goats. *Anim Feed Sci Tech*. 2020;262: 114410.
24. Wu J, Zhang X, Wang M, et al. Enhancing metabolic efficiency through optimizing metabolizable protein profile in a time progressive manner with weaned goats as a model: involvement of gut microbiota. *Microbiol Spectr*. 2022;10:10.
25. Lopes KP, Snijders GJL, Humphrey J, et al. Genetic analysis of the human microglial transcriptome across brain regions, aging and disease pathologies. *Nat Genet*. 2022;54:4–17.
26. Chen P, Xu H, Tang H, et al. Modulation of gut mucosal microbiota as a mechanism of probiotics-based adjunctive therapy for ulcerative colitis. *Microb Biotechnol*. 2020;13:2032–43.
27. Esther CR Jr, Muhlebach MS, Ehre C, et al. Mucus accumulation in the lungs precedes structural changes and infection in children with cystic fibrosis. *Sci Transl Med*. 2019;11: eaav3488.
28. Edgar RC. Search and clustering orders of magnitude faster than BLAST. *Bioinformatics*. 2010;26:2460–1.
29. Bolger AM, Lohse M, Usadel B. Trimmomatic: a flexible trimmer for Illumina sequence data. *Bioinformatics*. 2014;30:2114–20.
30. Li D, Liu C, Luo R, et al. MEGAHIT: an ultra-fast single-node solution for large and complex metagenomics assembly via succinct de Bruijn graph. *Bioinformatics*. 2015;31:3.
31. Benjamin B, Xie C, Huson DH. Fast and sensitive protein alignment using DIAMOND. *Nat Methods*. 2015;12:2.
32. Wu YW, Tang YH, Tringe SG, et al. MaxBin: an automated binning method to recover individual genomes from metagenomes using an expectation-maximization algorithm. *Microbiome*. 2014;2:2.
33. Kang DD, Li F, Kirton E, et al. MetaBAT 2: an adaptive binning algorithm for robust and efficient genome reconstruction from metagenome assemblies. *Peer J*. 2019;26: e7359.
34. Alneberg J, Bjarnason BS, Bruijn Id, et al. Binning metagenomic contigs by coverage and composition. *Nat Methods*. 2014;11:3.
35. Lin L, Lai Z, Zhang J, et al. The gastrointestinal microbiome in dairy cattle is constrained by the deterministic driver of the region and the modified effect of diet. *Microbiome*. 2023;11:10.
36. Sieber CMK, Probst AJ, Sharrar A, et al. Recovery of genomes from metagenomes via a dereplication, aggregation and scoring strategy. *Nat Microbiol*. 2018;3:3.
37. Hyatt D, Chen GL, LoCascio PF, et al. Prodigal: prokaryotic gene recognition and translation initiation site identification. *BMC Bioinformatics*. 2010;11: 119.
38. Rinke C, Chuvochina M, Mussig AJ, et al. A standardized archaeal taxonomy for the genome taxonomy database. *Nat Microbiol*. 2021;6:14.
39. Uritskiy GV, DiRuggiero J, Taylor J. MetaWRAP a flexible pipeline for genome-resolved metagenomic data analysis. *Microbiome*. 2018;6:6.
40. Asnicar F, Thomas AM, Beghini F, et al. Precise phylogenetic analysis of microbial isolates and genomes from metagenomes using PhyloPhlAn 3.0. *Nat Commun*. 2020;11:2500.
41. Letunic I, Bork P. Interactive Tree Of Life (iTOL) v4: recent updates and new developments. *Nucleic Acids Res*. 2019;47:256–9.
42. Chen H, Zhang YPJ. Enzymatic regeneration and conservation of ATP: challenges and opportunities. *Crit Rev Biotechnol*. 2021;41(1):16–33.
43. Hackmann TJ, Firkins JL. Electron transport phosphorylation in rumen butyrylviros: unprecedented ATP yield for glucose fermentation to butyrate. *Front Microbiol*. 2015;6:622.
44. Gill SK, Rossi M, Bajka B, et al. Dietary fiber in gastrointestinal health and disease. *Nat Rev Gastroenterol Hepatol*. 2021;18:101–16.
45. Han X, Ma Y, Ding S, et al. Regulation of dietary fiber on intestinal microorganisms and its effects on animal health. *Anim Nutr*. 2023;14:356–69.
46. Koh A, De Vadder F, Kovatcheva-Datchary P, et al. From dietary fiber to host physiology: short-chain fatty acids as key bacterial metabolites. *Cell*. 2016;165:1332–45.
47. Li ZJ, Wang XN, Zhang Y, et al. Genomic insights into the phylogeny and biomass-degrading enzymes of rumen ciliates. *ISME J*. 2022;16(12):2775–87.
48. Peng X, Wilken SE, Lankiewicz TS, et al. Genomic and functional analyses of fungal and bacterial consortia that enable lignocellulose breakdown in goat gut microbiomes. *Nat Microbiol*. 2021;6:499–511.
49. Li MM, White RR, Guan LL, et al. Metatranscriptomic analyses reveal ruminal pH regulates fiber degradation and fermentation by shifting the microbial community and gene expression of carbohydrate-active enzymes. *Anim Microbiome*. 2021;3(1):32.
50. Zhang Z, Xu D, Wang L, et al. Convergent evolution of rumen microbiomes in high-altitude mammals. *Curr Biol*. 2016;26:1873–9.
51. Guo N, Wu Q, Shi F, et al. Seasonal dynamics of diet gut microbiota interaction in adaptation of yaks to life at high altitude. *npj Biofilms Microb*. 2021;7:38.
52. Jonathan MC, van den Borne JJGC, van Wiechen P, et al. In vitro fermentation of 12 dietary fibres by faecal inoculum from pigs and humans. *Food Chem*. 2012;133:889–97.
53. Suarez BJ, Vann Reenen CG, Beldman G, et al. Effects of supplementing concentrates differing in carbohydrate composition in veal calf diets: I. animal performance and rumen fermentation characteristics. *J Dairy Sci*. 2006;89:43365–4375.

54. Cao W, Guan S, Yuan Y et al. The digestive behavior of pectin in human gastrointestinal tract: a review on fermentation characteristics and degradation mechanism. *Crit Rev Food Sci Nutr.* 2023; 64:1–24.
55. Marounek M, Dusikova D. Metabolism of pectin in rumen bacteria *Butyrivibrio fibrisolvens* and *Prevotella ruminicola*. *Lett Appl Microbiol.* 1999;29:429–33.
56. Hoover WH. Digestion and absorption in hindgut of ruminants. *J Anim Sci.* 1978;46:1789–99.
57. Jiao J, Wu J, Zhou C, et al. Ecological niches and assembly dynamics of diverse microbial consortia in the gastrointestinal of goat kids. *ISME J.* 2024;18(1):wrae002.
58. Xie F, Jin W, Si H, et al. An integrated gene catalog and over 10,000 metagenome-assembled genomes from the gastrointestinal microbiome of ruminants. *Microbiome.* 2021;9:137.
59. Dao MC, Everard A, Aron-Wisniewsky J, et al. *Akkermansia muciniphila* and improved metabolic health during a dietary intervention in obesity: relationship with gut microbiome richness and ecology. *Gut.* 2016;65(3):426–36.
60. Schoelmerich MC, Katsyv A, Doing J, et al. Energy conservation involving 2 respiratory circuits. *P Natl Acad Sci USA.* 2020;117(2):1167–73.
61. Mulkidjanian AY, Makarova KS, Galperin MY, et al. Inventing the dynamo machine: the evolution of the F-type and V-type ATPases. *Nat Rev Microbiol.* 2007;5:892–9.
62. Schep DG, Zhao J, Rubinstein JL. Models for the a subunits of the *Thermus thermophilus* V/A-ATPase and *Saccharomyces cerevisiae* V-ATPase enzymes by cryo-EM and evolutionary covariance. *P Natl Acad Sci USA.* 2016;113:3245–50.
63. Degnan PH, Taga ME, Goodman AL. Vitamin B₁₂ as a modulator of gut microbial ecology. *Cell Metab.* 2014;20:769–78.
64. Seshadri R, Leahy SC, Attwood GT, et al. Cultivation and sequencing of rumen microbiome members from the Hungate1000 Collection. *Nat Biotechnol.* 2018;36:359–67.

Publisher's Note

Springer Nature remains neutral with regard to jurisdictional claims in published maps and institutional affiliations.